DELAY TIME MODEL FOR TANDEM CYLINDER VIBRATION

Charles W. Knisely, Lecturer
Hiroji Nakagawa, Professor

Department of Civil Engineering, Kyoto University

1. INTRODUCTION

In many different applications, examples of closely spaced tandem structures with circular cross-section which are exposed to a mean velocity or current can be found. In the area of hydraulics, pier supports (pilings), underwater cables, submerged pipeline bundles and the risers on an offshore oil platform are a few examples. Examples from wind engineering include closely spaced smokestacks, radio and television towers, distillation columns, storage tanks for oil or water, electrical power cables and closely spaced pipe racks. In the mechanical sciences, one immediately thinks of heat exchangers as an example of this type of geometry.

It is important to recognize that all of these diverse geometries in their often different environments are susceptible to flow-induced vibrations. In the following, the symbols L and T will be used to denote the center-to-center spacing in the streamwise and transverse directions, respectively, U signifies the freestream velocity, f_c is the frequency of cylinder vibration, T_c is the period of vibration ($T_c = 1/f_c$) and D represents the cylinder diameter. Tandem cylinder vibrations can be excited by a variety of mechanisms, depending mainly on the L/D ratio.

Cooper and Wardlaw [1971] reported that when L/D > 5, the downstream cylinder can undergo what is termed "wake galloping" or "wake flutter". This type of vibration occurs when the reduced velocity, U/f_cD, exceeds a threshold value, known as the critical onset reduced velocity. The vibration of the downstream cylinder, characterized by elliptical orbits, is driven by the mean velocity gradients in the wake of the upstream cylinder.

A different type of oscillation can result when the cylinder spacing exceeds about six diameters (L/D > 6). If the downstream structure has an eigenfrequency near the vortex shedding frequency of the upstream structure, the impinging von Karman vortices from the upstream structure can cause a resonant vibration of the downstream structure. This type of vibration is termed "resonant buffeting" and has been examined by Wong [1980]. As with all vortex-induced vibrations one must expect that resonant buffeting will occur only over a limited reduced velocity range.

King and Johns [1976] investigated what they called "in-line proximity interaction" which can occur when the inter-cylinder spacing is less than six diameters (L/D < 6) and the mass damping parameter $k_s < 1.2$. The mass damping parameter is defined as $k_s = 2m_e\delta/\rho D^2$, where m_e is the modal mass, δ the logarithmic decrement and ρ the fluid density. This type of tandem cylinder interaction is usually limited to reduced velocities in the range $1.2 < U_R < 5$ and is characterized by cylinder motion in the flow direction.

"Cross-stream proximity interference galloping" or simply "interference galloping" has been discussed by many authors, among them Zdravkovich [1974], Zdravkovich and Pridden [1977], Ruscheweyh [1983] and most recently Shiraishi et al [1986]. This type of cross-stream vibration generally occurs when the spacing ratio is less than four (L/D < 4). Amplitudes of vibration are typically of the order of one diameter and vibrations can occur over a wide range of reduced velocities, nominally $30 < U_R <$ 100 to 200. The remainder of the present paper will deal with this "interference galloping" phenomenon.

Bokaian and Geoola [1984a,b] attempted to calculate the response of the downstream cylinder by assuming the forces acting on it were the same as those acting on a cylinder with a similar static displacement. The results of their quasi-steady analysis only faintly resembled their experimental data, indicating that the quasi-steady model is not appropriate. Ruscheweyh [1983] also employed a quasi-steady analysis, but he incorporated a phase shift between the cylinder motion and the resultant quasi-steady forces. His analytical results were in acceptable agreement with his empirical data.

The mechanism which drives interference galloping is thought to be the periodic switching of high speed flow into and out of the gap between the two cylinders. When the two cylinders are aligned in the streamwise direction, there is only recirculating flow in the gap between the two cylinders and their common wake is symmetrical. In the aligned position the transverse displacement of the downstream cylinder, η, is defined to be zero. As the downstream cylinder moves away from the centerline, that is, $|\eta| > 0$, it forces the wake to become unsymmetrical. At some critical transverse location, the downstream cylinder presents a large enough flow obstruction to force the shear layer emanating from the upstream cylinder to bend into the gap between the two cylinders. The area of this gap is relatively small and the resultant gap flow has a high velocity. The induced pressure field acts to restore the cylinder to its in-line arrangement, but the kinetic energy of the cylinder reaches a maximum just as it passes through the position corresponding to $\eta = 0$, and the cylinder's momentum carries the cylinder to a displaced position on the opposite side where the switching of high speed fluid, called "jet-switching" by Naudascher [1983], occurs once again.

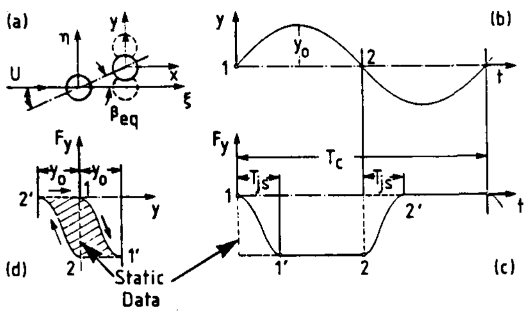

Fig. 1: Proposed mechanism for sustaining the oscillation of two closely spaced cylinders, after Knisely [1985].

The physical significance of the phase shift in Ruscheweyh's [1983] model, or, equivalently, a time delay between cylinder displacement and the equivalent quasi-steady loading, is presented in Fig. 1. In Fig. 1a the coordinate systems, (ξ,η) and (x,y), and the equilibrium position of the cylinder are defined. Note that for simplicity, the equilibrium position of the cylinder is at the critical transverse displacement ($\xi = L$, $\eta = T$) just prior to the occurrence of "jet-switching". This position is also given by β_{eq}, where $\beta_{eq} = \tan^{-1}(T/L)$. It is also assumed, again for simplicity, that the downstream cylinder undergoes harmonic oscillations as shown in Fig. 1b. The force on the downstream cylinder is dominated by the gap flow. When the high speed "jet" flow occurs there is a negative lift force exerted on the downstream cylinder. When there is only recirculating flow, the net lift force is approximately zero. The static lift force is idealized as a step function as shown by the dashed line in Fig. 1c and d. The switching of the "jet" into and out of the gap requires a finite amount of time due to the fluid inertia. The transverse lift force acting on the downstream cylinder is expected to be similar to the idealized curve shown as the solid line in Fig. 1c. The finite time required for the jet to switch into and that required for it to switch out of the gap are assumed to be approximately equal and are denoted by T_{js}. The significance of this delay time is evident in the force-displacement diagram in Fig. 1d. If the "jet switching" were instantaneous, the process would follow the line marked "static data" and the net area under the force-displacement curve would be exactly zero. The finite delay time results, however, in a closed loop which is traversed in a clockwise direction indicating energy transfer from the mean flow to the cylinder motion, thereby sustaining the cylinder vibration.

The experiments discussed in this paper were undertaken to crudely estimate an appropriate value for the delay time. After presentation of the delay time measurements, a delay time model for cylinder interaction is formulated and initial results are presented.

2. APPARATUS

Since the force on the downstream cylinder is dominated by the switching of the "jet" into and out of the gap, and since the instrumentation required for force measurement was unavailable, the experimental set-up shown in Fig. 2 was adopted. The downstream cylinder was forced to oscillate by means of a scotch yoke mechanism and the hot-film probe, mounted with the moving cylinder in a water flow, recorded the switching of the "jet" into and out of the gap. The placement of the hot-film probe was critical. After very careful observation using dye injection, the position shown in Fig. 2, 43° from the forward stagnation point (in uniform flow), was chosen.

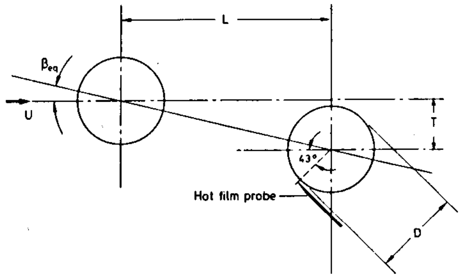

Fig.2: Experimental set-up for delay time measurement.

The errors associated with this choice will be discussed in the section of this paper entitled "Results".

Both cylinders were of diameter D = 5 cm. The value of L was held constant at 1.5D and T was −0.28D, resulting in an angle of β_{eq} = 10.6° (see Fig. 1) between their line of centers and the direction of the flow. The Reynolds number for all experiments reported here was 8.5 x 10^3. The frequency of forced vibration of the downstream cylinder was continuously variable, permitting reduced velocities, $U_R = U/(f_c D)$, over the range $5 < U_R < 50$. The amplitude of vibration could be varied continuously from 0 to 0.47D. The nominal water depth for the experiments was 20 cm, yielding a cylinder aspect ratio of 4. The channel was 50 cm wide, resulting in 10% blockage. No correction for blockage effects has been made.

All velocity measurements were made using a DISA 55M10 anemometer in conjunction with a DISA 55M25 linearizer and a conical hot film probe. The freestream streamwise velocity fluctuations were about 1% and the flow was uniform to within about one percent over the central 60% of the channel. Further details of the flow conditions can be found in Knisely [1985].

Dynamic measurements were obtained using a Hewlett Packard 5451C Fourier Analyzer to phase average the velocity signal. The cylinder displacement signal, obtained from a variable inductance LDVT, was used as a phase reference. Normally 40 samples were used to determine the ensemble average. The contribution of the probe's own velocity to the output signal was checked and found to be negligible above a reduced velocity of 7. Again, details can be found in Knisely [1985].

3. RESULTS

A typical example of the ensemble averaged gap velocity and cylinder displacement signals is given in Fig. 3. Positive cylinder displacement is toward the top of the page, as shown in Figs. 1 and 2. From Fig. 3 one can clearly see the delay time between the cylinder motion and the gap velocity. This delay time can be estimated by measuring directly from the time traces or by autocorrelating the two ensemble averaged time signals since only a single predominant frequency component is involved.

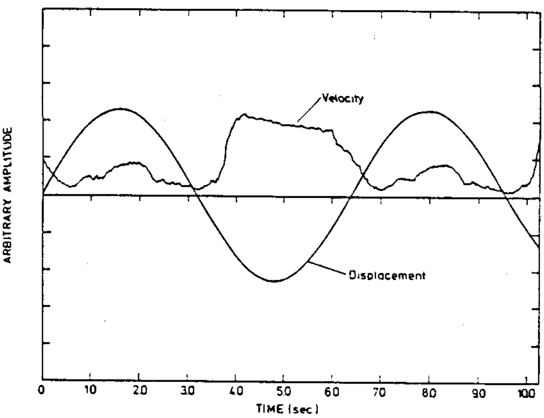

Fig. 3: Ensemble averaged dynamic gap velocity signal and cylinder displacement. L/D = 1.5, T/D = 0.28, U_R = 16.5, A/D = 0.47.

The results of the measurement of delay time required for the "jet" to switch into the gap for five different amplitudes of vibration and a range of reduced velocities is given in Fig. 4. Similar results were obtained for the time required for the jet to switch out of the gap. The data in Fig. 4 are well described by a linear correlation over the range of reduced velocities considered in the experiments. The correlations with a linear least squares curve fit are typically of the order of 90% or better. The worst fit and most scatter occurs when the amplitude of forced vibration is in the range 0.19D to 0.30D. Flow visualization revealed that in this amplitude range, the "jet" was formed by flow that first started around the outside of the downstream cylinder, but was subsequently forced to reverse direction and flow through the gap. The "jet flow" was attached to the downstream cylinder as it passed the forward stagnation point (in uniform flow), but separated before it passed the hot film probe located at 43°. For this reason, the data for A/D = 0.19 and 0.30 are somewhat scattered. The dependence of the delay time on the details of the flow introduces considerable error. The delay time data presented here are only estimates and may vary as much as ±20%.

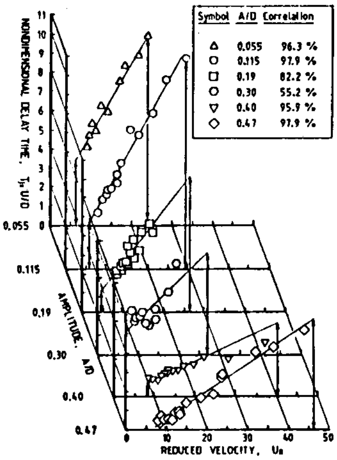

Fig. 4: Delay time for "jet switching" into the gap as a function of reduced velocity for A/D = 0.47, 0.40, 0.30, 0.21, 0.11 and 0.055.

The delay time is clearly a function of the amplitude as well as the reduced velocity of the flow. Preliminary results from additional experiments now in progress covering Reynolds numbers in the range 2×10^4 to 8×10^4 suggest there is a strong dependence of the delay time on Reynolds number, as well. Rigorously, the delay times presented in Fig. 4 are valid only for a Reynolds number of 8.5×10^3.

To arrive at a single correlation curve, the least squares curve fits to the data for the average delay times, $(T_{switching\ in} + T_{switching\ out})/2$, were replotted in many different forms, using the convenience of Lotus 123 software to quickly plot the various combinations of parameters. The form that best correlated the data, and also made the most sense physically, is shown in Fig. 5, where the nondimensional delay time is plotted as a function of the reduced velocity divided by the square root of the nondimensional amplitude of vibration. The quantity $U_R(A/D)^{-0.5}$ can also be written as $(U/\sqrt{D})(f_c^2 A)^{-0.5}$ and can be considered to represent the maximum nondimensional cylinder acceleration. Note that the systematic variation of delay time with amplitude of vibration, found in Fig. 4, has disappeared in Fig. 5. The curves for A/D = 0.055, 0.3 and 0.47 are almost identical. The deviation of the other curves is most likely due to the details of the gap flow, that is, local separations. The errors involved in measuring the switching time in the manner employed here may be considerable, but the data does suggest that correlating the delay time with the parameter $U_R(A/D)^{-0.5}$ may be fruitful. The following nondimensional correlation has been assumed, based on the data in Fig. 5:

$$\tau_{js} = T_{js}\, U/G = k_D\, (U/D)\, (f_c^2 A/D)^{-0.5} \quad (1)$$

where k_D is a nondimensional coefficient and the variable G has been substituted for D as the characteristic length. G is a measure of the approximate length of the free shear layer emanating from the upstream cylinder and is given by:

$$G = D\{(L/D)^2 + (T/D)^2 - T/D + 0.25\}^{0.5} \quad (2)$$

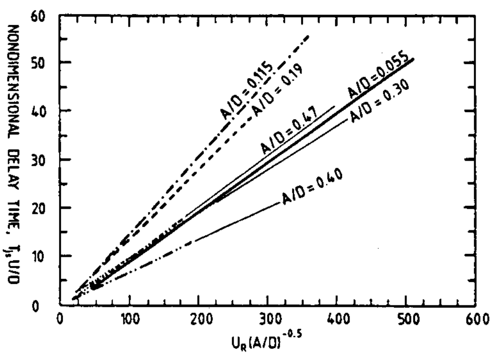

Fig. 5: Delay time vs. nondimensional acceleration parameter.

The value for the constant k_D will later be determined by a trial and error procedure so that the calculated results match the experimental laboratory results at a single point, i.e. at Re = 1×10^5. The test of the model then is whether the rest of the calculated data correspond to the experimentally determined trends.

Employing Eq. (2) and recalling that $4\pi^2 f_c^2 A$ is equal to the maximum cylinder acceleration (for harmonic motion) one can arrive at the following correlation for the dimensional delay time:

$$T_{js} = k_D\, (G^2/D)^{0.5}\, |\ddot{y}_{max}/(4\pi^2)|^{-0.5} \quad (3)$$

As mentioned previously, experiments

currently in progress at Kyoto University suggest that k_D is a function of Reynolds number. Since the Reynolds number dependence was unknown at the time of the present analysis, however, the above correlation for T_D, Eq. (3), was employed in the delay time model of tandem cylinder proximity galloping. More refined calculations will be undertaken after this Reynolds number dependence is quantified.

4. EQUATION OF MOTION

The equation of motion for the downstream cylinder can be written as that of a simple forced oscillator, provided the cylinder vibrates as a rigid body, that is, the mode shape is given by $\psi = 1$. The forcing term on the right-hand side is the net flow-induced force per unit length in the y-direction. The equation of motion is

$$m\ddot{y} + c\dot{y} + ky = L(t) - C_D(0.5\rho\dot{y}^2 D) \quad (4)$$

where it is assumed that L(t) can be given by the equivalent static force evaluated at a delay time T_{js}. Thus $L(t) = F(\xi,\eta^*)$ where F is the force corresponding to a static displacement and $\eta^* = \eta(t - T_{js})$.

Knowledge of the initial conditions and the static force distribution for static displacements, that is $F(\xi,\eta)$, coupled with the delay time model, Eq.(3) permits the solution of the equation of motion, Eq. (4), at least in theory.

5. NUMERICAL SOLUTION

The delay time inherent in the evaluation of L(t) causes significant problems if one attempts to solve Eq. (4). By assuming a starting cycle of undamped harmonic motion, the flow-induced force at negative times can be estimated for the start of the problem. The initial assumption is that the motion is nearly periodic, as was observed in the laboratory studies of Zdravkovich [1974]. The procedure is to neglect all damping and flow-induced forces and calculate one period of vibration of the undamped system. After one period of vibration, the cylinder is again at its original starting point with the same initial velocity and the same initial displacement. Rigorously this solution procedure is not valid, but as an engineering approximation for a process that is known to be almost periodic it may yield reasonable results.

The static lift distributions presented by Zdravkovich and Pridden [1977] for Re = 6 x 10^4 were employed for the solution of the equation of motion. Analytical expressions were developed that closely resembled the static lift coefficient distribution, although these expressions did not match the empirical data exactly.

The second order problem was rewritten as two coupled first order equations and these were integrated using the Euler method. There is much room for refinement and optimization of the numerical techniques. The results presented here are intended to demonstrate that the delay time formulation does indeed lead to oscillatory behavior that follows the trends of the laboratory results of Zdravkovich [1974].

The solution program was written in BASIC and calculations were carried out on a KAYPRO PC, an IBM compatible personal computer. The results are plotted as phase plane trajectories.

The calculated test cases were intended to emulate the experiments of Zdravkovich [1974]. In his paper, the exact mass, spring forces and damping are not presented, rather the natural frequency and the damping factor are presented. By making crude estimates concerning the density of the material he employed it was possible to examine a number of cases that should come close to his conditions, but no attempt was made to match the experimental data by adjusting the mass in the calculations.

Unless otherwise noted, the results presented below are for an assumed mass per unit length of 2.0 kg, with a damping factor of 11.3 kg/s and a spring constant of 280 N/m. The delay time used in the calculations was determined from Eq. (3) as long as U_R was less than 80. For higher values of U_R, the delay time was assumed to remain constant at the value corresponding to U_R = 80. The value of k_D used in the calculations was 0.215.

There is considerable concern that the method of solution will lead to results which are a function of the initial conditions. Fig. 6 shows the limit cycle in the phase plane for two different initial conditions. In Fig. 6a the limit cycle is approached from below while in Fig. 6b the same limit cycle is approached from above.

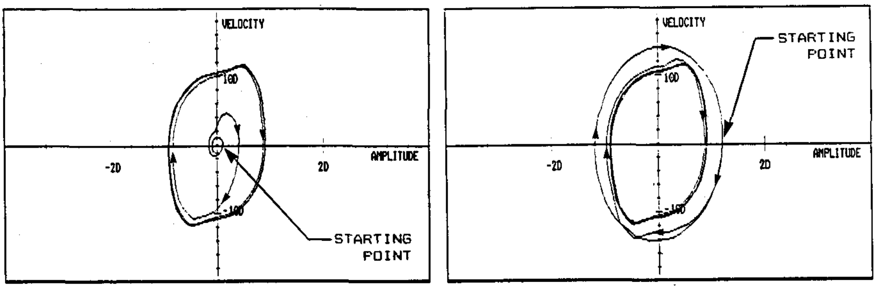

Fig. 6: Demonstration of independence of limit cycle from initial conditions. Calculations for m = 5 kg, c = 28 kg/s and k = 700 N/m.

The results of calculations for variation with L/D and Reynolds number, neglecting any variation in k_D with Re, are shown in comparison with Zdravkovich's [1974] laboratory data in Fig. 7. While the calculated results do not agree exactly in magnitude with the experimental results, the general trends are quite similar. Based on these preliminary findings, it would appear worthwhile to pursue this line of research. With necessary adjustments for variation in delay time and static lift coefficients with Reynolds number and numerical refinement, the proposed method may lead to an acceptable prediction of the proximity galloping of tandem cylinders.

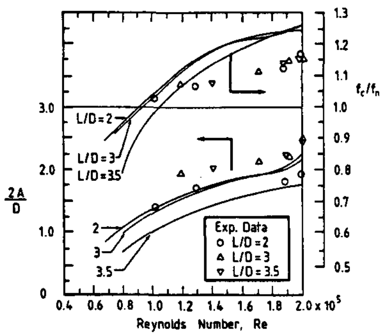

Fig. 7: Comparison of calculated results with experimental data from Zdravkovich [1974]. Upper curve is frequency ratio and lower curve reduced double amplitude.

6. CONCLUSION

From measurement of the kinematic jet switching time, a delay time model for proximity galloping of tandem cylinders has been formulated. The preliminary solution of the equation of motion for the downstream cylinder employing this delay time model yielded results of the correct magnitude that agreed with the general trend of the laboratory results of Zdravkovich [1974]. Further refinement of the model and the numerical techniques are required before the amplitudes and frequencies of vibration can be predicted exactly.

7. REFERENCES

Bokaian, A. and Geoola, F. 1984a. **J. Fluid Mech. 146**, 383-415.

Bokaian, A. and Geoola, F. 1984b. **J. Fluid Mech. 146**, 417-449.

Cooper, K.R. and Wardlaw, R.L. 1971. Proc. 3rd Internat. Conf. on Wind Effects on Buildings and Structures, Tokyo, 647-655.

King, R. and Johns, D.J. 1976. **J. Sound Vib. 45**, 259-283.

Knisely, C. 1985. "Flow Visualization and the Kinematics of Tandem Cylinder Interaction," Report SFB 210/E/15, Sonderforschungsbereich 210, University of Karlsruhe, Karlsruhe, W. Germany.

Naudascher, E. 1983. Engineering for Structures Subject to Flow-Induced Forces and Vibrations (Notes from Intensive Course), 11-13 January, University of Karlsruhe, Karlsruhe, W. Germany.

Ruscheweyh, H. 1983. **J. Wind Eng. and Industrial Aero. 14**, 129-140.

Shiraishi, N., Matsumoto, M. and Shirato, H. 1986. **J. Wind Eng. and Industrial Aero. 23**, 437-447.

Wong, H.Y. 1980. **J. Wind Eng. and Industrial Aero. 6**, 49-57.

Zdravkovich, M.M. 1974. Proc. IUTAM/IAHR Symposium on Flow-Induced Vibrations, Karlsruhe, Springer Verlag, Berlin, 631-639.

Zdravkovich, M.M. and Pridden, D.L. 1977. J. Wind Eng. and Industrial Aero. **2**, 255-270.